

Optimization-based design of surface textures for thin-film Si solar cells

Xing Sheng,^{1,*} Steven G. Johnson,² Jurgen Michel,¹ and Lionel C. Kimerling¹

¹Department of Materials Science and Engineering, Massachusetts Institute of Technology, Cambridge, Massachusetts 02139, USA

²Department of Mathematics, Massachusetts Institute of Technology, Cambridge, Massachusetts, 02139 USA
*shengx@mit.edu

Abstract: We numerically investigate the light-absorption behavior of thin-film silicon for normal-incident light, using surface textures to enhance absorption. We consider a variety of texture designs, such as simple periodic gratings and commercial random textures, and examine arbitrary irregular periodic textures designed by multi-parameter optimization. Deep and high-index-contrast textures exhibit strong anisotropic scattering that is outside the regime of validity of the Lambertian models commonly used to describe texture-induced absorption enhancement for normal incidence. Over a 900–1100 nm wavelength range, our optimized surface texture in two dimensions (2D) enhances absorption by a factor of $2.7\pi n$, considerably larger than the original πn Lambertian result and exceeding by almost 50% a recent generalization of Lambertian model for periodic structures in finite spectral range. However, the πn Lambertian limit still applies for isotropic incident light, and our structure obeys this limit when averaged over all the angles. Therefore, our design can be thought of optimizing the angle/enhancement tradeoff for periodic textures.

©2011 Optical Society of America

OCIS codes: (040.5350) Photovoltaic.

References and links

1. R. Brendel, *Thin-Film Crystalline Silicon Solar Cells: Physics and Technology* (Wiley-VCH Verlag GmbH & Co. KGaA, Weinheim, 2003).
2. J. Poortmans and V. Arkhipov, *Thin Film Solar Cells: Fabrication, Characterization and Applications* (John Wiley & Sons, Ltd, 2006).
3. P. Sheng, A. N. Bloch, and R. S. Stepleman, "Wavelength-selective absorption enhancement in thin-film solar cells," *Appl. Phys. Lett.* **43**(6), 579–581 (1983), <http://link.aip.org/link/doi/10.1063/1.94432>.
4. C. Heine and R. H. Morf, "Submicrometer gratings for solar energy applications," *Appl. Opt.* **34**(14), 2476–2482 (1995), <http://www.opticsinfobase.org/abstract.cfm?URI=ao-34-14-2476>.
5. L. Zeng, Y. Yi, C. Hong, J. Liu, N. Feng, X. Duan, L. C. Kimerling, and B. A. Alamariu, "Efficiency enhancement in Si solar cells by textured photonic crystal back reflector," *Appl. Phys. Lett.* **89**(11), 111111 (2006), <http://link.aip.org/link/doi/10.1063/1.2349845>.
6. N. N. Feng, J. Michel, L. Zeng, J. Liu, C. Y. Hong, L. C. Kimerling, and X. Duan, "Design of highly efficient light-trapping structures for thin-film crystalline silicon solar cells," *IEEE Trans. Electron Devices* **54**, 1926–1933 (2007), <http://dx.doi.org/10.1109/TED.2007.900976>.
7. P. Bermel, C. Luo, L. Zeng, L. C. Kimerling, and J. D. Joannopoulos, "Improving thin-film crystalline silicon solar cell efficiencies with photonic crystals," *Opt. Express* **15**(25), 16986–17000 (2007), <http://www.opticsinfobase.org/abstract.cfm?URI=oe-15-25-16986>.
8. C. Haase and H. Stiebig, "Thin-film silicon solar cells with efficient periodic light trapping texture," *Appl. Phys. Lett.* **91**(6), 061116–061119 (2007), <http://link.aip.org/link/doi/10.1063/1.2768882>.
9. J. G. Mutitu, S. Shi, C. Chen, T. Creazzo, A. Barnett, C. Honsberg, and D. W. Prather, "Thin film solar cell design based on photonic crystal and diffractive grating structures," *Opt. Express* **16**(19), 15238–15248 (2008), <http://www.opticsinfobase.org/abstract.cfm?URI=oe-16-19-15238>.
10. P. G. O'Brien, N. P. Kherani, A. Chutinan, G. A. Ozin, S. John, and S. Zukotynski, "Silicon Photovoltaics Using Conducting Photonic Crystal Back-Reflectors," *Adv. Mater. (Deerfield Beach Fla.)* **20**(8), 1577–1582 (2008), <http://dx.doi.org/10.1002/adma.200702219>.
11. L. Zeng, P. Bermel, Y. Yi, B. A. Alamariu, K. A. Broderick, J. Liu, C. Hong, X. Duan, J. D. Joannopoulos, and L. C. Kimerling, "Demonstration of enhanced absorption in thin film Si solar cells with textured photonic crystal back reflector," *Appl. Phys. Lett.* **93**(22), 221105 (2008), <http://link.aip.org/link/doi/10.1063/1.3039787>.

12. R. Dewan, M. Marinkovic, R. Noriega, S. Phadke, A. Salleo, and D. Knipp, "Light trapping in thin-film silicon solar cells with submicron surface texture," *Opt. Express* **17**(25), 23058–23065 (2009), <http://www.opticsinfobase.org/abstract.cfm?URI=oe-17-25-23058>.
13. J. Zhu, C. M. Hsu, Z. Yu, S. Fan, and Y. Cui, "Nanodome solar cells with efficient light management and self-cleaning," *Nano Lett.* **10**(6), 1979–1984 (2010), <http://dx.doi.org/10.1021/nl9034237>.
14. S. B. Mallick, M. Agrawal, and P. Peumans, "Optimal light trapping in ultra-thin photonic crystal crystalline silicon solar cells," *Opt. Express* **18**(6), 5691–5706 (2010), <http://www.opticsinfobase.org/abstract.cfm?URI=oe-18-6-5691>.
15. S. E. Han and G. Chen, "Toward the Lambertian limit of light trapping in thin nanostructured silicon solar cells," *Nano Lett.* **10**(11), 4692–4696 (2010), <http://dx.doi.org/10.1021/nl1029804>.
16. X. Sheng, J. Liu, N. Coronel, A. M. Agarwal, J. Michel, and L. C. Kimerling, "Integration of Self-Assembled Porous Alumina and Distributed Bragg Reflector for Light Trapping in Si Photovoltaic Devices," *IEEE Photon. Tech. Lett.* **22**, 1394–1396 (2010), <http://dx.doi.org/10.1109/LPT.2010.2060717>.
17. A. Naqavi, K. Soderström, F.-J. Haug, V. Paeder, T. Scharf, H. P. Herzig, and C. Ballif, "Understanding of photocurrent enhancement in real thin film solar cells: towards optimal one-dimensional gratings," *Opt. Express* **19**(1), 128–140 (2011), <http://www.opticsinfobase.org/abstract.cfm?URI=oe-19-1-128>.
18. X. Sheng, J. Liu, I. Kozinsky, A. M. Agarwal, J. Michel, and L. C. Kimerling, "Design and non-lithographic fabrication of light trapping structures for thin film silicon solar cells," *Adv. Mater. (Deerfield Beach Fla.)* **23**(7), 843–847 (2011), <http://dx.doi.org/10.1002/adma.201003217>.
19. C. Lin and M. L. Povinelli, "Optical absorption enhancement in silicon nanowire arrays with a large lattice constant for photovoltaic applications," *Opt. Express* **17**(22), 19371–19381 (2009), <http://www.opticsinfobase.org/oe/abstract.cfm?URI=oe-17-22-19371>.
20. A. Lin and J. Phillips, "Optimization of random diffraction gratings in thin-film solar cells using genetic algorithms," *Sol. Energy Mater. Sol. Cells* **92**(12), 1689–1696 (2008), <http://dx.doi.org/10.1016/j.solmat.2008.07.021>.
21. V. E. Ferry, M. A. Verschuuren, H. B. T. Li, R. E. I. Schropp, H. A. Atwater, and A. Polman, "Improved red-response in thin film a-Si:H solar cells with soft-imprinted plasmonic back reflectors," *Appl. Phys. Lett.* **95**(18), 183503 (2009), <http://link.aip.org/link/doi/10.1063/1.3256187>.
22. O. Isabella, F. Moll, J. Krc, and M. Zeman, "Modulated surface textures using zinc-oxide films for solar cells applications," *Phys. Status Solidi A* **207**, 642–646 (2010), <http://dx.doi.org/10.1002/pssa.200982828>.
23. Z. Yu, A. Raman, and S. Fan, "Fundamental limit of nanophotonic light trapping in solar cells," *Proc. Natl. Acad. Sci. U.S.A.* **107**(41), 17491–17496 (2010), <http://dx.doi.org/10.1073/pnas.1008296107>.
24. Z. Yu, A. Raman, and S. Fan, "Fundamental limit of light trapping in grating structures," *Opt. Express* **18**(S3 Suppl 3), A366–A380 (2010), <http://www.opticsinfobase.org/oe/abstract.cfm?URI=oe-18-S3-A366>.
25. C. Lin and M. L. Povinelli, "The effect of plasmonic particles on solar absorption in vertically aligned silicon nanowire arrays," *Appl. Phys. Lett.* **97**(7), 071110 (2010), <http://link.aip.org/link/doi/10.1063/1.3475484>.
26. E. Yablonovitch, "Statistical ray optics," *J. Opt. Soc. Am.* **72**(7), 899–907 (1982), <http://www.opticsinfobase.org/abstract.cfm?URI=josa-72-7-899>.
27. K. Sato, Y. Gotoh, Y. Wakayama, Y. Hayasahi, K. Adachi, and H. Nishimura, "Highly textured SnO₂:F TCO films for a-Si solar cells," *Rep. Res. Lab. Asahi Glass Co. Ltd.* **42**, 129–137 (1992).
28. H. R. Stuart and D. G. Hall, "Thermodynamic limit to light trapping in thin planar structures," *J. Opt. Soc. Am. A* **14**(11), 3001–3008 (1997), <http://www.opticsinfobase.org/abstract.cfm?URI=josaa-14-11-3001>.
29. Z. Yu and S. Fan, "Angular constraint on light-trapping absorption enhancement in solar cells," *Appl. Phys. Lett.* **98**(1), 011106 (2011), <http://link.aip.org/link/doi/10.1063/1.3532099>.
30. J. D. Joannopoulos, S. G. Johnson, J. N. Winn, and R. D. Meade, *Photonic Crystals: Molding the Flow of Light*, 2nd ed. (Princeton University Press, 2008).
31. J. M. Gee, "Optically enhanced absorption in thin silicon layers using photonic crystals," in *Proceedings of 29th IEEE Photovoltaic Specialists Conference* (Institute of Electrical and Electronics Engineers, New Orleans, LA, 2002), pp. 150–153, <http://dx.doi.org/10.1109/PVSC.2002.1190478>.
32. J. Wang, J. Hu, X. Sun, A. Agarwal, and L. C. Kimerling, "Cavity-enhanced multispectral photodetector using phase-tuned propagation: theory and design," *Opt. Lett.* **35**(5), 742–744 (2010), <http://www.opticsinfobase.org/abstract.cfm?URI=ol-35-5-742>.
33. M. Ghebrebrhan, P. Bermel, Y. Avniel, J. D. Joannopoulos, and S. G. Johnson, "Global optimization of silicon photovoltaic cell front coatings," *Opt. Express* **17**(9), 7505–7518 (2009), <http://www.opticsinfobase.org/abstract.cfm?URI=oe-17-9-7505>.
34. P. Campbell and M. Green, "The limiting efficiency of silicon solar cells under concentrated sunlight," *IEEE Trans. Electron Devices* **33**, 234–239 (1986), <http://dx.doi.org/10.1109/T-ED.1986.22472>.
35. A. Taflove and S. C. Hagness, *Computational Electrodynamics*, 2nd ed. (Artech House, Norwood, MA, 2000).
36. A. F. Oskooi, D. Roundy, M. Ibanescu, P. Bermel, J. D. Joannopoulos, and S. G. Johnson, "MEEP: A flexible free-software package for electromagnetic simulations by the FDTD method," *Comp. Phys. Comm.* **181**, 687–702 (2010), <http://dx.doi.org/10.1016/j.cpc.2009.11.008>.
37. S. G. Johnson, *The NLOpt nonlinear-optimization package*, <http://ab-initio.mit.edu/nlopt>.
38. M. J. D. Powell, "Direct search algorithms for optimization calculations," *Acta. Numerica* **7**, 287–336 (1998), <http://dx.doi.org/10.1017/S0962492900002841>.
39. T. P. Runarsson and X. Yao, "Search biases in constrained evolutionary optimization," *IEEE Trans. Syst. Man Cybern. C: Appl. Rev.* **35**, 233–243 (2005), <http://dx.doi.org/10.1109/TSMCC.2004.841906>.
40. W. C. Chew, J. M. Jin, E. Michielssen, and J. Song, eds., *Fast and Efficient Algorithms in Computational Electromagnetics* (Artech House, Norwood, MA, 2001).

41. G. Strang, *Computational Science and Engineering* (Wellesley-Cambridge Press, Wellesley, MA, 2007).
42. D. C. Dobson and S. J. Cox, "Maximizing Band Gaps in Two-Dimensional Photonic Crystals," *SIAM J. Appl. Math.* **59**(6), 2108–2120 (1999), <http://dx.doi.org/10.1137/S0036139998338455>.
43. P. Borel, A. Harpøth, L. Frandsen, M. Kristensen, P. Shi, J. Jensen, and O. Sigmund, "Topology optimization and fabrication of photonic crystal structures," *Opt. Express* **12**(9), 1996–2001 (2004), <http://www.opticsinfobase.org/oe/abstract.cfm?URI=oe-12-9-1996>.
44. C. Y. Kao, S. Osher, and E. Yablonovitch, "Maximizing band gaps in two-dimensional photonic crystals by using level set methods," *Appl. Phys. B* **81**(2-3), 235–244 (2005), <http://dx.doi.org/10.1007/s00340-005-1877-3>.
45. W. R. Frei, D. A. Tortorelli, and H. T. Johnson, "Topology optimization of a photonic crystal waveguide termination to maximize directional emission," *Appl. Phys. Lett.* **86**(11), 111114 (2005), <http://link.aip.org/link/doi/10.1063/1.1885170>.
46. Y. Tsuji and K. Hirayama, "Design of Optical Circuit Devices Using Topology Optimization Method With Function-Expansion-Based Refractive Index Distribution," *IEEE Phot. Tech. Lett.* **20**, 982–984 (2008), <http://dx.doi.org/10.1109/LPT.2008.922921>.

1. Introduction

In this paper, we use numerical optimization of surface textures to improve the efficiency of thin-film silicon photovoltaics—a promising technology for solar energy due to their low-cost large-scale manufacturability [1, 2], but for which a major challenge is to absorb light at infrared wavelengths where the absorption length is much larger than the active layer thickness. Previously we and others proposed and experimentally demonstrated the effectiveness of using deterministic periodic structures as promising solutions for efficiency enhancement [3–18]. Front and/or back surface textures (whether periodic or aperiodic) [3–24] can improve efficiency by scattering normally incident light into the plane of the film, but are limited by the fact that the same texture also scatters in-plane light back out of the film. In order to understand these limits, various authors have considered textured-surface absorption under models with restricted assumptions for which an explicit limit can be derived. The most well-known models are the Lambertian models [26], which consider surface textures under the key assumptions of isotropic scattering, in which case the efficiency enhancement is at most πn in 2D or $4n^2$ in 3D for a film (with index n) of infinite thickness and spectral range. More recently Yu et al. [24] showed that for a thin film over a wavelength range from λ_1 to λ_2 the best Lambertian enhancement is increased to $\pi n(1 + \lambda_1/\lambda_2)$ for 2D periodic structures at normal incidence. It is known that higher efficiency can be achieved in angular-sensitive devices [29], however, and we show how this enhancement/sensitivity tradeoff can be optimized while remaining in the context of periodic thin-film textures. In particular, we consider normally incident light on a Si thin film, backed by a textured SiO₂ layer and a reflecting mirror as shown in Fig. 1, in two dimensions for simplicity. A large amplitude of surface texture will not be an isotropic scatterer, and we show that even simple periodic textures like the sawtooth grating can exceed Yu's generalized Lambertian results. We also show that symmetric gratings, like the triangular grating, lose approximately a factor of 2 in performance as predicted by Ref. [24], and we show that considerably worse performance is achieved by random texture of commercial Asahi glass [27]. We apply multi-parameter optimization to a general texture, described by an arbitrary Fourier series, to obtain the best performance to date: enhancement 50% larger than Yu's limit (and even larger efficiency may be possible as the particular set of optimized parameters only represents a local optimum rather than a global one). However, our structure still obeys the fundamental Lambertian limit derived for isotropic input light [29], and in that sense optimizes the tradeoff between enhancement and angular sensitivity for periodic textures.

Lambertian models were pioneered by Yablonovitch [26], who considered absorption in a thick slab ($d \gg \lambda$) by surface texturing in an ergodic ray-optics regime over infinite spectral range, and showed that a $4n^2$ limits on absorption results in 3D, and a similar result was shown by Stuart and Hall [28] under an isotropic scattering assumption in the wave optics regime. In 2D, the corresponding limit was shown to be πn [24]. Specifically, for a film of thickness d and absorption coefficient α , the dimensionless absorption enhancement factor F is defined to be:

$$F = \frac{1}{\lambda_2 - \lambda_1} \int_{\lambda_1}^{\lambda_2} A(\lambda) d\lambda \quad (1)$$

where $A(\lambda)$ is fraction of light absorbed by the structure at each wavelength, averaging over a range from λ_1 to λ_2 . The $4n^2$ and πn results were recently extended to normal incidence on periodic textures with finite thicknesses and finite spectral range by Yu et al. [24], who modeled the film by a set of guided-wave resonances; they assumed isotropic scattering by assuming that each resonance radiates equally into all the channels. (They also implicitly assumed weak scattering, in that the leaky-mode description of resonances is only valid if the resonances decay slowly. On the other hand, they assumed that the radiative scattering occurs much more quickly than absorption). They showed that the πn limit in a periodic 2D structure could be increased by a factor of 2 at a single wavelength under these assumptions, and when their result is averaged over a finite spectral range one obtains a $\pi n(1 + \lambda_1/\lambda_2)$ enhancement for an “optimal” grating period $A = \lambda_1$. This result in their model is achieved for asymmetric textures like the sawtooth grating in Fig. 1, whereas they argue that symmetric textures (like the triangular grating in Fig. 1) lose a factor of 2 in efficiency because normal-incident light can only couple to half of the guided-wave resonances (the symmetric resonances) [4, 24].

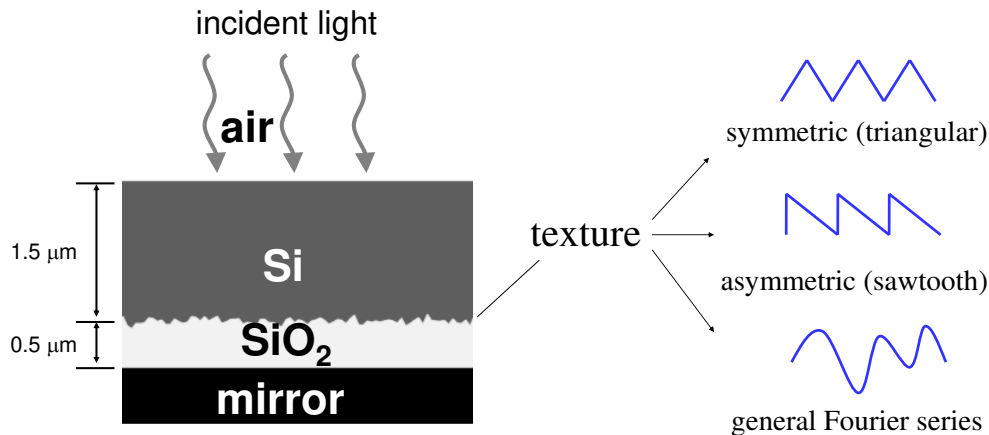


Fig. 1. (left) Schematic device structure for a thin-film Si solar cell with a textured Si / SiO₂ interface. The averaged thicknesses for Si and SiO₂ layers are 1.5 μm and 0.5 μm, respectively. (right) Different types of texture we investigate are symmetric triangular grating, asymmetric sawtooth grating and general periodic structures with Fourier series.

However, it is known that these $4n^2$ and πn factors are not fundamental limits if one considers incident light over only a narrow range of angles and wavelengths. More fundamental Lambertian limits were proved for the case of isotropic incident light—in this case, without any restriction to isotropic scatterers, it was proved that the angle-averaged enhancement is at most πn in 2D and $4n^2$ in 3D, assuming that the absorbing layer is thick enough to be described by the local density of states of the uniform material [29]. If the incident angles are restricted to lie within $[-\theta, \theta]$, then it was argued that the enhancement bound is instead $4n^2/\sin^2\theta$ (for 3D) or $\pi n/\sin\theta$ (for 2D) [34]. If one is willing to restrict consideration to a limited range of angles, therefore, the question is then how one can achieve this enhancement in practice. Over a very narrow spectral range, one can use planar (non-textured) surfaces to design a resonant mode achieving nearly 100% absorption (arbitrarily large enhancement as the absorption coefficient vanishes) by Q -matching (impedance matching) [30–33], although this requires a spectral range of at most the inverse of the

absorption lifetime. Over a much larger spectral range, one could conceivably use a large lens to concentrate the incident light onto a small spot, an idea used in various solar concentrator designs [34]. On the other hand, the situation is less clear if one has a large spectral range but restricts oneself to wavelength-scale periodic textures, in order to have translation-invariant performance (unlike a lens), e.g. to enable large areas or to have a very thin device. One can certainly design periodic or other textures to respond resonantly to normal-incident light, but as the incident angle is changed one would normally expect these resonances to shift continuously in frequency, so that many resonances will still lie within the bandwidth over some range of angles. To optimally exploit a narrow range of incident angles, while retaining a relatively large spectral range and a periodic texture, one needs to somehow achieve resonances that not only shift rapidly with angle but also rapidly alter their lifetimes or amplitudes. One therefore clearly needs a texture that scatters very anisotropically so as to be angle-sensitive, in which case the isotropic Lambertian models for normal-incident light no longer apply. In order to fully explore these tradeoffs in the absence of analytical Lambertian models, one ultimately requires large scale optimization to explore the large space of texture parameters.

2. Computational method

The 2D device structure used in our numerical model is illustrated in Fig. 1. From top to bottom, it consists of air (semi-infinite), 1.5 μm crystalline silicon (Si), 0.5 μm silicon dioxide (SiO_2) and a perfect reflector on the backside. For the sake of simplicity, electrical components like metal grids or transparent conductive oxides (TCOs) are not included in the optical model. Meanwhile, the silicon is considered to be intrinsic and the effects of p and n regions are neglected. The front surface of silicon and the interface between SiO_2 and reflector are kept flat, and only the interface between Si and SiO_2 are textured. It should be noted that the volumes of Si and SiO_2 are kept constant when different type of textures are evaluated. That means, if the texture is characterized by a function $H(x)$, we enforce that the average H_{avg} is held constant at 0.5 μm .

To simulate this structure, we employ a finite-difference time-domain (FDTD) method [35] implemented via an open source code Meep [36]. The simulation cell size is Λ in the x direction, with a periodic boundary condition for normal incident light and a grid resolution of 10 nm. The material refractive indices are 3.6 for Si and 1.4 for SiO_2 . The Si layer is assumed to be weakly absorptive, with a constant absorption coefficient ($\alpha = 12.56 \text{ cm}^{-1}$) between 900 nm and 1100 nm (implemented as a constant conductivity). In this wavelength range, the unit cell is illuminated under normal incidence by TE polarized light (with the electric field perpendicular to the plane) in the spectral range from 900 nm to 1100 nm. The absorption spectrum $A(\lambda)$ is calculated by Fourier-transforming the response to a short pulse to obtain $A = 1 - \text{reflection}$, with a wavelength resolution of 1 nm. The performance of the texture is characterized by the dimensionless enhancement factor F of Eq. (1), which is the averaged absorption divided by the single-pass absorption αd . Different light-trapping structures are simulated and compared in terms of their performance F . For this wavelength range (from 900 nm to 1100 nm), Yu's model [24] predicts an optimal F of $1.8\pi n$ for $\Lambda = 900$ nm with asymmetric textures, and an optimal $F = \pi n$ for $\Lambda \rightarrow \infty$ with symmetric textures. This theory is verified by simulating a shallow grating in our model.

3. Simulation results

3.1 Light trapping by Asahi glass

The first type of structure we investigate is from commercially available Asahi U-type glass [27], which is a glass plate coated by fluorine doped tin oxide ($\text{SnO}_2:\text{F}$). It is widely used as a superstrate for amorphous and microcrystalline silicon solar cells. The intentionally textured $\text{SnO}_2:\text{F}$ works as a conductive layer as well as a scattering layer for light trapping. We measured the surface morphology of an Asahi glass sample by an atomic force microscope (AFM), and calculated the root-mean-square (RMS) roughness to be 30 nm. To construct a

2D model for comparison, 1D textures were extracted from the measured AFM image and imported into the model mentioned in Fig. 1. To obtain a more accurate result, 20 different 1D textures (with a length of 4000 nm) were arbitrarily selected and simulated, and we computed enhancement factors F from $0.90\pi n$ to $1.28\pi n$ (average $(1.04 \pm 0.10)\pi n$), which are very close to the prediction of a conventional 2D Lambertian surface ($F = \pi n$) [24].

3.2 Light trapping by symmetric triangular gratings

Diffraction gratings have been proposed as promising candidates to improve solar cell efficiency [3–18]. Here we implement a symmetric triangular grating into our model (Fig. 2a), and investigate its influences on light trapping. Absorption-enhancement factors F are calculated based on the simulated absorption spectra (from 900 nm to 1100 nm), and plotted as a function of the grating period Λ and thickness t . As shown in Fig. 2b, the optimal regions are around $\Lambda = 900$ nm, although there also are other parameters shown to have high absorption. Figure 2c shows the absorption spectrum of the optimal structure indicated in Fig. 2b ($\Lambda = 920$ nm and $t = 520$ nm). The calculated maximum F is $1.26\pi n$, which exceeds the value πn predicted by the Yu's model for symmetric gratings [24].

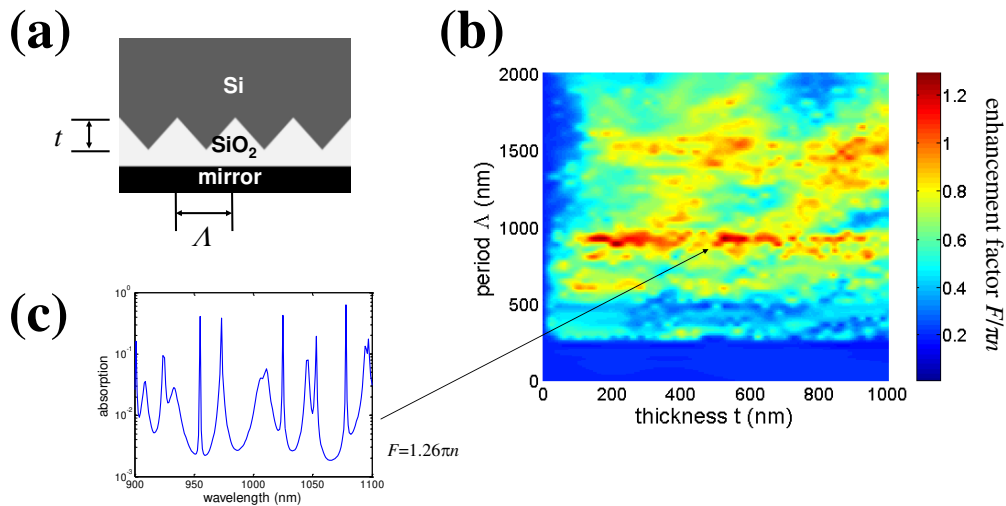


Fig. 2. (a) Schematic device structure with symmetric triangular grating. (b) Plot of the absorption enhancement factor (F) as a function of the grating period Λ and thickness t . The arrow indicates the optimal parameters. (c) Absorption spectrum of the optimal structure ($\Lambda = 920$ nm and $t = 520$ nm), obtaining $F = 1.26\pi n$.

3.3 Light trapping by asymmetric sawtooth gratings

We now investigate the performance of an asymmetric sawtooth grating (Fig. 3a), following the inspiration that asymmetry should enhance performance for normal incidence [4, 24]. Similar to Section 3.2, the enhancement factor F is plotted as a function of Λ and t in Fig. 3b. Optimal regions are still around $\Lambda = 900$ nm; however, F is significantly higher than that obtained for symmetric grating, with a maximum value of $2.04\pi n$. Again, this result exceeds the value $1.8\pi n$ predicted by Yu's model for asymmetric gratings [24]. The optimal structure has $\Lambda = 920$ nm and $t = 240$ nm. As illustrated in Fig. 3c, the absorption spectrum for the optimized sawtooth grating has many more resonance peaks than the optimized symmetric grating (Fig. 2c), which causes a larger enhancement. This is because in structures with mirror symmetry (Fig. 2a), normally incident plane wave can only couple to even modes while resonances with odd modes remain unexcited [4, 24].

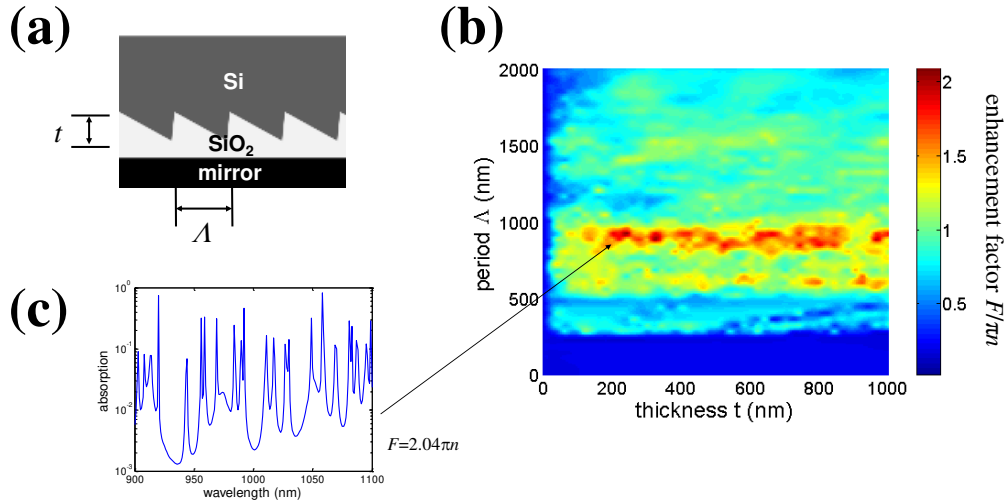


Fig. 3. (a) Schematic device structure with asymmetric sawtooth grating. (b) Plot of the absorption enhancement factor (F) as a function of the grating period Λ and thickness t . The arrow indicates the optimal parameters. (c) Absorption spectrum of the optimal structure ($\Lambda = 920$ nm and $t = 240$ nm), obtaining $F = 2.04\pi n$.

3.4 Light trapping by grating with optimized Fourier series

To further explore the light trapping limit of a periodic structure, an arbitrarily shaped texture should be studied. In principle, any arbitrarily shaped periodic texture, described by the function $H(x)$ (in nanometers), can be expanded in terms of its Fourier series:

$$H(x) = 500 + \sum_{n=1}^{\infty} \left(A_n \sin\left(\frac{2\pi n}{\Lambda} x\right) + B_n \cos\left(\frac{2\pi n}{\Lambda} x\right) \right) \quad (2)$$

where 500 nm is the averaged thickness of SiO₂ layer (the volume of SiO₂ is fixed), and Λ is the period of the simulation cell. To ensure that the texture does not cross the SiO₂ / mirror interface, we use a constraint $|H(x) - 500| < 500$. Because the absorption can be numerically calculated for any given device texture $H(x)$, the enhancement factor F is directly related to the Fourier coefficients ($A_1, B_1, A_2, B_2, \dots$) and period Λ :

$$F = F(A_1, B_1, A_2, B_2, \dots, \Lambda) \quad (3)$$

Therefore, we can optimize the device performance F by tuning the parameters ($A_1, B_1, A_2, B_2, \dots$ and Λ). As a practical matter, the number of parameters is limited by the simulation capability. We choose the first 5 orders as degrees of freedom, i.e. from (A_1, B_1) to (A_5, B_5), and set higher-order Fourier coefficients to zero. One of those parameters is redundant for periodic boundary condition, because it corresponds to a phase shift. Therefore, we can set $B_5 = 0$ without loss of generality. Based on previous results in Section 3.2 and 3.3 as well as the prediction of Yu's model [24], we expect that the optimal structure has a period of around 900 nm, so we choose the initial Λ to be 900 nm, but Λ is permitted to be varied in the optimization. The FDTD method is combined with a nonlinear optimization toolbox NLOpt [37]. The algorithm we use is based on constrained optimization by linear approximation (COBYLA) [38]. Generally, this problem may have many local optima, and it is infeasible to guarantee that the global optimum has been obtained, so these local optima only represent a lower bound on the attainable performance. We also explored the use of a genetic global-optimization algorithm [39], but its convergence rate was so slow that over feasible run times it obtained inferior results than repeated local optimization. We run the optimization several times with different initial parameter values to explore different local optima. In 3 runs, we achieve optimized enhancement factors (F) of $2.07\pi n$, $2.10\pi n$ and $2.28\pi n$, respectively. These

local optima are noticeably larger than the prediction of the Yu's model [24]. In addition, the optimizations keep Λ close to its initial value of 900 nm.

In our model, textured Si/SiO₂ interface is the critical component introducing strong anisotropic scattering, while the magnitude of the surface roughness is determined by the thickness of the silicon oxide layer. Therefore, to further explore the light trapping limit, we introduce the oxide thickness t_{ox} as an additional parameter for optimization. With this additional parameter, we achieve optimized enhancements F of $2.28\pi n$, $2.38\pi n$ and $2.70\pi n$, which are even higher than the obtained results when t_{ox} was fixed at 500nm in the previous simulations. The best found parameters are listed in Table 1, with a calculated $F = 2.70\pi n$, which is 50% larger than the prediction of the Yu's model ($F = 1.8\pi n$). Of course, it is possible that other local optima exist with even better performance.

The above method explores light trapping performances for asymmetric structures, since it includes both sine and cosine coefficients. By using only cosine coefficients, we can also optimize symmetric structures. Here we intentionally set all the sine coefficients (A_1 to A_5) to zeros. We obtain optimized F of $1.56\pi n$, $1.45\pi n$ and $1.36\pi n$, respectively. The performances of optimized symmetric structures are much lower than those achieved for asymmetric structures, but still larger than the prediction of the Yu's model [24] and are also larger than the performance of the optimized triangular grating.

Table 1. Optimized Structural Parameters For Asymmetric Structures, With $F = 2.70\pi n$. The Units For $A_1, B_1, A_2, B_2 \dots t_{\text{ox}}$ And Λ Are nm. B_5 Is Set To A Constant 0.

A_1	B_1	A_2	B_2	A_3	B_3	A_4	B_4	A_5	B_5	Λ	t_{ox}	$F/\pi n$
256	-44.1	36.1	82.2	-22.1	93.1	218	-44.4	-43.7	0	882	666	2.70

3.5 Comparison and discussion

Our simulation results are compared with the generalized Lambertian model by Yu et al. [24]. As mentioned in the introduction, the enhancement factor F for 2D period- Λ structures in this Lambertian model is:

$$F(\Lambda) = \frac{1}{\lambda_2 - \lambda_1} \int_{\lambda_1}^{\lambda_2} \left(\frac{\frac{\Lambda}{\lambda}}{\left\lfloor \frac{\Lambda}{\lambda} \right\rfloor + \frac{1}{2}} \right) d\lambda \cdot \pi n \quad \text{for asymmetric structures} \quad (4)$$

and

$$F(\Lambda) = \frac{1}{\lambda_2 - \lambda_1} \int_{\lambda_1}^{\lambda_2} \left(\frac{\frac{\Lambda}{\lambda}}{\left\lfloor \frac{\Lambda}{\lambda} \right\rfloor + 1} \right) d\lambda \cdot \pi n \quad \text{for symmetric structures} \quad (5)$$

In Ref.24, F is plotted for a single wavelength λ , whereas here we average over a given range from $\lambda_1 = 900$ nm to $\lambda_2 = 1100$ nm. As shown in Fig. 4 (in green), this maximum F occurs when $\Lambda = 900$ nm, in which $F = 1.8\pi n$ for asymmetric structures. For symmetric structures, $F = 0.90\pi n$ for the first maximum, but approaches πn as Λ goes to infinity. As we mention in Section 3.1, textures from commercial Asahi glass (the dotted line in black) show performance close to πn .

Performances of our simulated triangular and sawtooth gratings are also shown in Fig. 4 (in blue). Here we select and plot the largest F at each period Λ in Fig. 2b and Fig. 3b. As illustrated, both triangular grating and sawtooth grating follow a trend similar to the analytical models, peaking at around $\Lambda = 900$ nm. However, these simulated results F deviate from the Lambertian models, showing higher values for most periods.

In addition, we illustrate the results for gratings with optimized Fourier series in Fig. 4a (in black and red dots). Due to the computational expense of this optimization, we only plot

local optima for several runs with different initial values at $\Lambda \approx 900$ nm. Nevertheless, all of them exceed the optimal sawtooth gratings as well as the Lambertian models. The best Fourier structures are also illustrated in the insets, with $F = 2.70\pi n$ for asymmetric structures and $F = 1.56\pi n$ for symmetric structures. These results clearly demonstrate that violating the isotropic coupling assumption in Yu's model [24] can lead to higher performances.

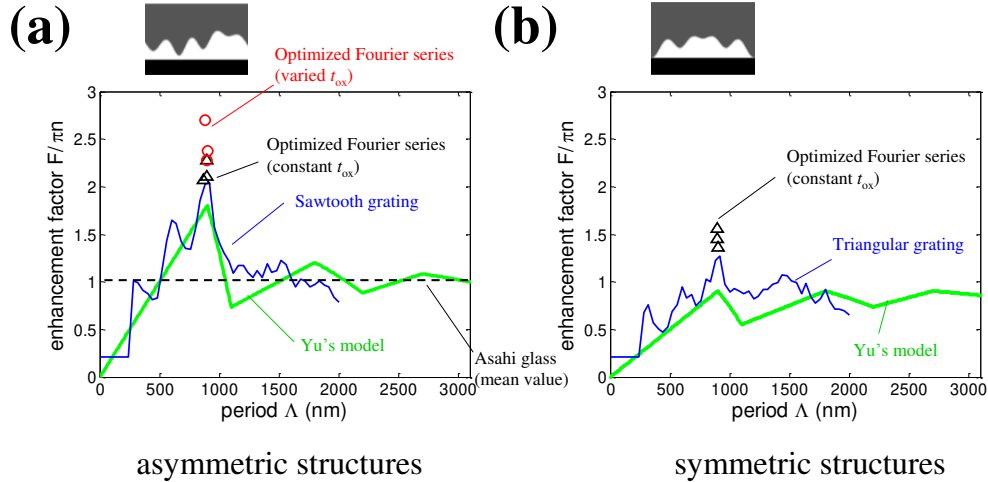


Fig. 4. Summary of the calculated maximum enhancement factors F in Section 3 and comparison with Yu's model in Ref [24], and commercial Asahi glass. The insets indicate the structures with the best performance achieved in our optimizations. (a) Asymmetric structures. (b) Symmetric structures.

3.5 Angular response of the optimized structure

As explained in the introduction, this super-Lambertian enhancement for normal incident light must necessarily come at the expense of enhancement at other angles. To demonstrate this, in Fig. 5 we plot the enhancement factor versus incident angle, as computed by a rigorous coupled wave analysis (RCWA) method [6]. As expected, the enhancement factor F decreases significantly for non-normal incidence [24]. F is larger than πn for incident angles within about $[-25^\circ, 25^\circ]$. The average enhancement factor over all angles

$$F_{avg} = \frac{1}{2} \int_{-\frac{\pi}{2}}^{\frac{\pi}{2}} F(\theta) \cos \theta d\theta \quad (5)$$

is calculated to be $0.9\pi n$, which still obeys the classical Lambertian limit for isotropic light [26, 29]. It should be noted that low-cost thin-film Si solar cells are usually implemented within a non-concentrated configuration like a roof-top system, so strictly restricting the angle range is not practical. Nevertheless, our design provides a methodology for achieving high efficiency solar cells with restricted angles. In addition, our design is still instructive for practical applications since the incoming power of sunlight is not isotropic and usually peaks in the middle of the day. Therefore, it is still meaningful to design a cell with a better performance for normal incidence.

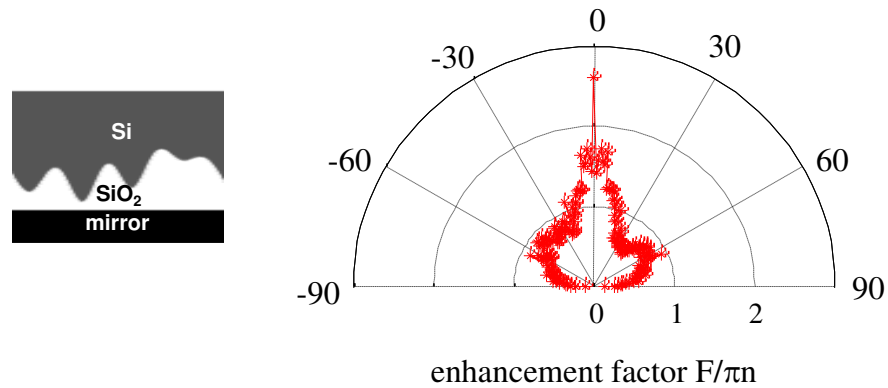


Fig. 5. Angular dependence of the optimized asymmetric structures obtained in Fig. 4a.

4. Conclusion

Lambertian models provide a simple and instructive intellectual framework for describing the effects of surface texturing on thin-film absorption. Even outside their range of validity (isotropic scattering), they can still be surprisingly descriptive: in our case, we find that the Lambertian prediction gives a rough guideline as to the optimal texture period, and is within 50% of the actual performance. In order to design an optimal texture structure at normal incidence, including strong anisotropic scattering, one must eventually depart from the confinements of analytical models, however beautiful, and resort to brute-force computation and parameter optimization. The results in this paper provide a glimpse of what is possible from such a computational approach, in which significant improvements are obtained even by a small number of local optimizations (despite the nonlinear and nonconvex nature of this optimization problem). Such local optima represent only lower bounds on the attainable performance, and by expending additional effort one could certainly envision pushing those bounds upwards, although locating the true global optimum with confidence seems daunting. It may also be possible to analytically prove more general upper bounds on performance for gratings with a given period and specific incident angle. As a practical matter, a more important goal is to adapt these techniques to 3D. In order to improve the efficiency of the calculation and make 3D optimization feasible, a number of techniques could be employed. First, one could use more sophisticated computational techniques than FDTD, such as boundary-element methods that only require the interfaces to be discretized [40]. Second, one could use adjoint methods to compute the gradient of F with respect to the optimization parameters [41], and thereby employ much more efficient gradient-based optimization methods (such methods have been used in topology optimization of photonic structures with hundreds or thousands of degrees of freedom [42–46]). As a heuristic method, it might be interesting to investigate using the optimized Fourier coefficients from the 2D simulations in this paper to form a two-dimensional texture with similar frequency components in 3D.

Acknowledgements

The authors would like to thank Mr. Yutian Lei, Dr. Peter Bermel and Prof. Juejun Hu for valuable discussions. This work was supported by Massachusetts Institute of Technology Energy Initiative (MITEI), and also supported in part by the AFOSR MURI for Complex and Robust On-chip Nanophotonics (G. Pomrenke, grant FA9550-09-1-0704).